

# New Lenses for Microlithography

Erhard Glatzel\*  
Mathematische Abteilung\*\*  
Carl Zeiss, Oberkochen

## Introduction

I should like to present new lenses for microlithography developed by Carl Zeiss, and try at first to summarize the optical design problem in simplified form. Nine lenses will then be discussed. Three are typical photographic lenses and six microlithography lenses with an image scale of 1:10, of which the last four items are of completely new design characterized by two strong bulges of the ray bundle, for which high-index glasses of poor transmission are not needed.

## The optical design problem

The correction of the *Petzval* sum, that is the flattening of the image field, is the basic problem in the design of photographic lenses. With respect to the problem I also refer to the article by Jan Hoogland [1].

The *Petzval* sum can be reduced by combining positive and negative lens elements as suggested, for instance, by Hermann Slevogt [2].

The properties of a specific lens are defined by the way these lens elements are combined.

Convergent elements produce *constrictions*, divergent *bulges* of the ray bundle. How this fact is utilized to correct the *Petzval* sum is easily understood.

If in the well-known relation

$$(1) \sum_i \frac{\varphi_i}{n_i}$$

where  $\varphi_i$  are the surface powers and  $n_i$  the refractive indices, it is required that:

$$(2) \sum_i \varphi_i$$

be as small as possible, = 0, or < 0.

In the following investigations I shall always use this approximation at first and then discuss the influence of the refractive indices on the exact relation of the *Petzval* sum. This procedure will reveal the great importance of this approximation.

Assuming a positive total refractive power which is normalized to one, another relation is known to apply:

$$(3) \sum_i F_i = 1.$$

where  $F_i = \omega_i \varphi_i$  are weighted surface powers, and  $\omega_i$  is the paraxial height ratio  $h_i : h_1$  of a ray which is incident parallel with the axis.

The design problem is the following: although a total refractive power must be produced, the sum of the individual surface powers should approach zero.

I am using here the term "weighted powers" introduced by Ludvik Čanžek [3].  $\omega_i$  are the weights, and  $F_i$  is the contribution of the  $i$ -th surface to the total refractive power.  $F_i$  and partial sums thereof are in this physical sense primary quantities of an optical system. The origin of the total refractive power should therefore be the first subject of investigation of every image aberration analysis.

As suggested by relations (2) and (3) a lens designer must try to achieve a high impact of the positive refractive powers. This calls for bulging of the ray bundle by preceding elements. Negative refractive powers should be provided where  $\omega$  is small, i.e. the bundle constricted. This can be realized only by preceding convergent lens elements.

A well-known means of correction is the provision of a field flattener where  $\omega$  is extremely small or zero.

The ways and means applied to achieve the favorable *Petzval* sum of tele lenses are known: the negative lens element is arranged far behind the positive element at a site where  $\omega$  is only about 0.3 to 0.5.

Also well-known are the classical lens designs with the characteristic strong constriction in the central part with values of  $\omega$  which range from 0.6 to 0.8. In lenses of the Triplet, Tessar, Planar type etc. the central part is followed by more or less extended bulges. These bulges may be omitted altogether as is generally the case in the Sonnar lenses.

Also known are lenses of the retrofocus type which feature a bulge followed by a constriction, yet rarely a second, considerably effective bulge. Long retrofocus lenses may have considerable first bulges, resulting in  $\omega$ -values of 2 and more.

Wide-angle lenses with divergent front and rear lens elements offer even better correction facilities.

Last but not least the combined effect of a positive and a negative surface power of a thick meniscus lens has a most favorable effect on the *Petzval* sum.

Such measures for bulging and constricting the ray bundle can be repeatedly employed. The effect is the more pronounced the greater the differences of the  $\omega$ -values. In other words: the stronger and more frequent bulges and constrictions, the easier the sum of all surface powers can be reduced to zero or below zero.

If  $\sum \varphi$  cannot be made sufficiently small, the last means available is the choice of the refractive indices. A high refractive index of the convergent lens elements, and a low index of the divergent ones will then have a favorable effect on the *Petzval* sum. However, if the refractive indices are employed to correct the *Petzval* sum, they are no longer available for the correction of other aberrations. The cemented surface of an old-achromat, for example, which is an excellent means to correct spherical aberration must then be abandoned.

Yet, when designing an optical system the influence of different refractive indices on the *Petzval* sum should not be overestimated, notwithstanding the fact that for the correction of a certain lens type higher refractive indices, especially of the convergent lens elements, are quite frequently the only means to achieve a better *Petzval* sum. The correction of the other aberrations does not permit further bulging or constriction of the ray bundle. The same is true when the ray bundle is less bulged or constricted in order to achieve a higher aperture.

## Typical constrictions and bulges

The weighted refractive powers are now compared with the surface powers by means of examples. An illustration is only possible when individual surfaces of the lenses are combined in groups. The first example (Fig. 1) is the Zeiss Planar f/1.4-50 mm for the 35 mm format as shown by Walter Wöltche [4] as well. The ray bundle is constricted and then bulged. (The scales of the illustrations are such that the physical lengths of the lenses can be directly compared).

Fig. 1 shows the combination of a convergent front group, a divergent central group, and a convergent rear group. The corresponding partial sums of the weighted powers (dashed arrows) and the partial sums of the refractive powers (solid arrows) are plotted underneath. The total sums (thick solid arrows) are shown to the right of the plot. The arrow for the total sum of the weighted powers is normalized to 1. The arrow for the total sum of the refractive powers should be zero, although this is not the case here. The sum of all surface powers amounts to +0.46, which is less than half the sum of the weighted powers. But even if all lens elements had the same high refrac-

\*Lecture held on May 5, 1980 at a Zeiss colloquium in Oberkochen, and read by Dr. Hannfried Zügge at the International Lens Design Conference in Oakland, Cal., USA on June 2, 1980. First published in English in SPIE, vol. 237 (1980), courtesy Society of Photo-Optical Instrumentation Engineers.

\*\*Mathematical Division

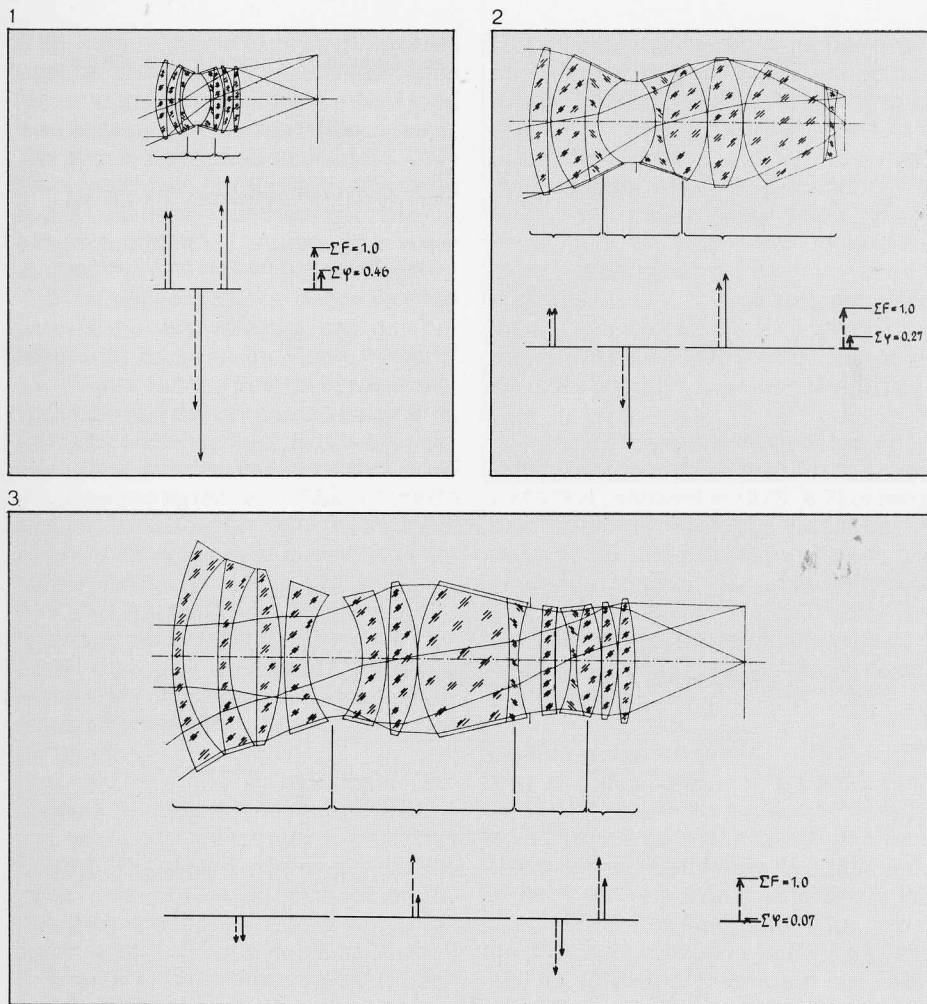


Fig. 1:  
Zeiss Planar  $f/1.4-50$  mm for the 24x36 mm format.

Fig. 2:  
Zeiss Planar  $f/0.7-50$  mm for 35 mm film.

Fig. 3:  
Zeiss Distagon  $f/1.2-18$  mm for 35 mm film.

Fig. 3 shows a retrofocus lens. Like the Zeiss Planar  $f/0.7-50$  mm it has been designed for the 35 mm movie film format. The overall length of this Zeiss Distagon  $f/1.2-18$  mm is more than twice that of the Planar lens discussed before, and amounts to 7.6f. Our new lenses for microlithography are of the same length. The Distagon is split up into four groups. (This is done for better illustration and to ease comparison. The grouping is reasonable but not binding).

The first group of the lens is divergent; the remaining part of the system has convergent power and consists of a second convergent, a third divergent, and a fourth convergent group. The first divergent group bulges the ray bundle sufficiently for the correction of the Petzval sum. The second group already produces the difference between weighted refractive power and refractive power of the total system. The third and fourth groups taken together do not noticeably contribute to the correction. From the third to the fourth group the bundle is weakly bulged. The refractive powers are considerable, but the distance between the elements is extremely short. This illustrates the importance of a divergent group in front for the bulge of the ray bundle.

This lens features an aspheric surface near the stop, which is, however, of minor importance for the discussion. With this aspheric surface certain surface powers can be reduced, and it also accounts in part for the extraordinarily low refractive powers. The lens is new and covered by a patent granted in 1977 [6]. The use of an aspheric surface and a great physical length – both means of correction were applied for this lens – correspond to my statements [7] at 1975's International Lens Design Conference in Haverford.

$\Sigma\phi = 0.07$  is already now less than the value 0.10 of the exact Petzval sum. Although the average refractive indices are still quite high, the value 1.67 of  $n_+$  falls for the first time below the value 1.74 of  $n_-$ . There is a great difference between the two values, which permits a jump of the refractive index of 0.29 with respect to the new diverging, curved cemented surface of the rear group. This offers a most valuable means of correction, indirectly created by the strong bulge of the front group. All examples mentioned below have been corrected accordingly.

tive index, the exact Petzval sum of 0.17, which is the correct value for this lens, is not attainable. Even with high refractive indices of 1.75 the Petzval sum would only be  $\frac{0.46}{1.75} = 0.26$ .

Consequently, the refractive indices of the convergent lens elements had to be higher than those of the divergent ones. In order to obtain simple quantities for the refractive indices and the amounts of refractive-index differences, an average refractive index  $n_+$  of the convergent lens elements and  $n_-$  of the divergent ones is defined as follows:

$$(4) \frac{1}{n_+} \sum \phi_i = \sum \frac{1}{n_i} \phi_i.$$

The sum considers all surfaces of convergent lens elements. The right side of the equation indicates the share of the convergent lens elements in the Petzval sum while the corresponding share of  $\Sigma\phi$  on the left side is divided by the average refractive index. Cemented surfaces are replaced by air spaces of zero thickness.

The average refractive index  $n_-$  of divergent lens elements is obtained in the same manner:

$$(5) \frac{1}{n_-} \sum \phi_i = \sum \frac{1}{n_i} \phi_i.$$

The sum considers all surfaces of divergent lens elements.

The average refractive indices of the Zeiss Planar  $f/1.4-50$  mm are:  $n_+ = 1.78$

and  $n_- = 1.72$ , which results in the exact Petzval sum of 0.17.

Let me now summarize the above. Constriction and bulging reduce the sum from 1 to 0.46, high refractive indices from 0.46 to 0.26, and the refractive-index differences from 0.26 to 0.17. The lens is of short design; its physical length amounts to only 0.8-times the focal length  $f$ . The overall length is 1.5f including the back focal distance. Refractive powers must be high to achieve the desired effect at short distances.

The next example (Fig. 2) is the Zeiss Planar  $f/0.7-50$  mm [5]. The lens is twice as long as the above-mentioned Planar and requires much lower refractive powers of the groups which are combined in accordance with Fig. 1. It contains a most effective, extremely divergent lens element directly in front of the image plane. This element has been included in the rear component for a better comparison with the examples below where such flattening lens elements are markedly less influential. Constriction and bulging of the ray bundle are more pronounced. The sum of all surface powers amounts to only 0.27. The exact Petzval sum is 0.10. The average refractive index of the convergent lens elements is 1.70. In this case it had to be provided so as to exceed the average refractive index of the divergent lens elements of 1.65.



## Lenses for Microlithography

Discussed below are diffraction-limited lenses for 10x reduction without vignetting. Carl Zeiss, Oberkochen have designed and manufactured such lenses for more than a decade. They are in use in the semiconductor industry for the production of masks or for direct projection onto wafers cut from a semiconductor crystal, e.g. silicon. They are intended to image largest possible fields at numerical apertures from 0.28 to 0.42.

The use of these lenses for direct projection onto wafers calls for greater depth of focus without any loss in image quality. This can be realized in diffraction-limited lenses only by correction for shorter wavelengths. When the aperture is reduced in proportion to the shortening of the wavelengths, the depth of focus increases in the same proportion. The modulation transfer function (MTF) is maintained. Thus  $\lambda/NA$  determines the minimum producible features. NA is the numerical aperture. The dimensions which are feasible in actual production amount to about 0.8-times this quantity, which requires special, partially coherent illumination (see also the paper by Bruce Irwing [8]).

Because of their poor transmission high-index glasses cannot be employed in the short wavelength range. Yet, high-index glasses were used for all lenses mentioned above and are preferable also for high-aperture, diffraction-limited lenses.

I should like to present a new lens type. For identical or even improved  $\lambda/NA$ -values classical low-index glass types are employed to correct these lenses with the result of satisfactory transmission even at the 365 nm wavelength. How this was achieved by bulging the ray bundle twice will be explained below. The new lens type is suitable for image scales of 1:10 and hitherto unattained image fields at comparable apertures, object-to-image distances, back focal distances and telecentric ray paths in the image space.

Let us now have a look at the development of this lens. We start with the lens shown in Fig. 4 which is used by David Mann and Elektromask in wafer steppers and mask repeaters with an object-to-image distance of 602 mm. I showed the lens and one of its predecessors in Haverford in 1975 [7]. All lens sections are normalized so that the object-to-image distance is the same for the 1:10 image scale, and diameter and physical length are directly comparable.

The Zeiss S-Planar f/1.6-50 mm (drawing No. 10 77 82) shown in Fig. 4 is still relatively small. Its numerical aperture is

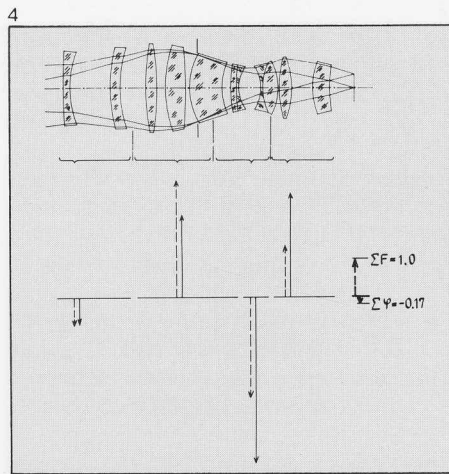


Fig. 4:  
Zeiss S-Planar f/1.6-50 mm for  $\lambda = 436$  nm.

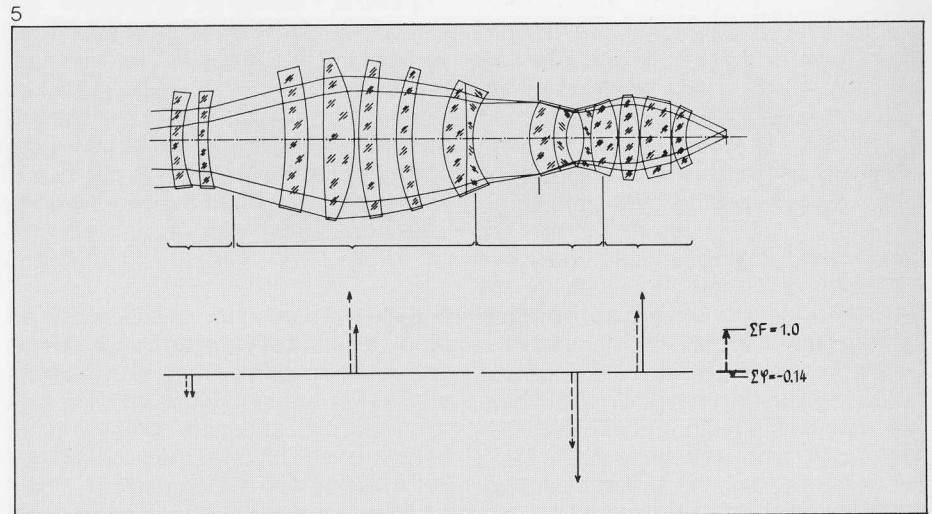


Fig. 5:  
Zeiss S-Planar f/1.1-42 mm for  $\lambda = 436$  nm.

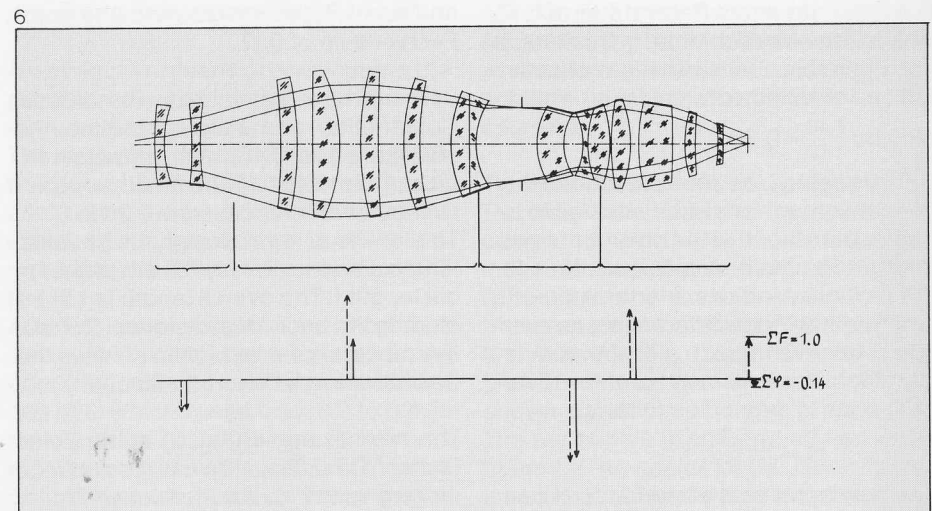


Fig. 6:  
Zeiss S-Planar f/1.3-65 mm for  $\lambda = 436$  nm.

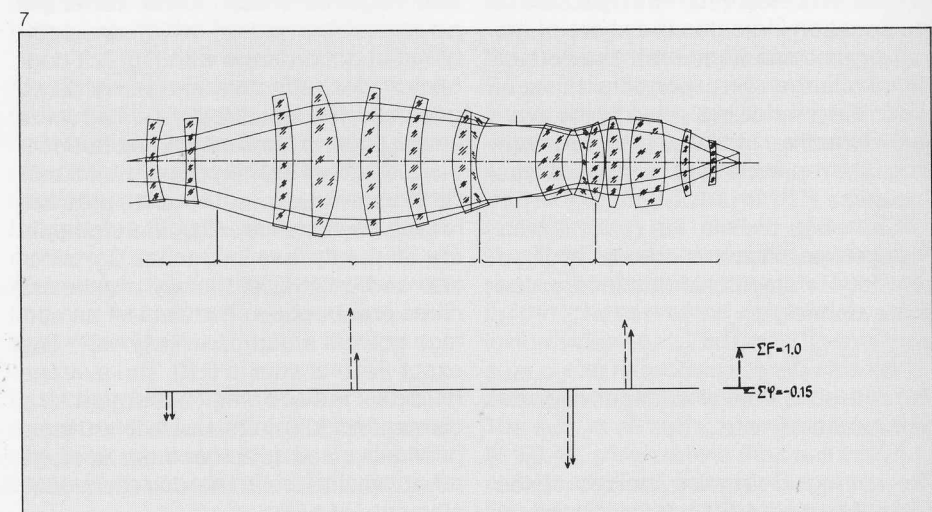


Fig. 7:  
Zeiss S-Planar f/1.3-36.5 mm for  $\lambda = 405$  nm.

0.28, the image field  $10 \times 10 \text{ mm}^2$ , and it is used at the 436 nm wavelength. This lens and the following items offer a long working distance in front of the image. The above-mentioned value of  $0.8 \lambda/\text{NA}$  amounts to  $1.25 \mu\text{m}$ . Exactly this value is guaranteed by David Mann for the minimum producible features of his wafer stepper.

The refractive powers and weighted powers are relatively high and comparable with those of the Zeiss Planar  $f/1.4\text{-}50 \text{ mm}$ . But the new lens type is distinguished by the ray bundle bulge in its front part with the effect of a clearly negative total sum of the refractive powers. Average refractive indices of the divergent lenses higher than those of the convergent ones were possible. Compared with the Zeiss Planar  $f/1.4\text{-}50 \text{ mm}$  this allowed reduced curvature of the divergent surfaces of the inner menisci.  $\Sigma\phi = -0.17$ ;  $n_+ = 1.65$  and  $n_- = 1.72$ . As with all lenses mentioned below the value of 0.03 of the Petzval sum is negligibly small.

The next lens (Fig. 5) has double the physical length and the refractive powers are correspondingly lower. This Zeiss S-Planar  $f/1.1\text{-}42 \text{ mm}$  is intended for an object-to-image distance of 602 mm. It is exceptional in that it has a high aperture of 0.42 but only a small field of  $5 \times 5 \text{ mm}^2$ . It is the forerunner of the following double-bulge lenses, and its lens section was shown by Gerhard Ittner [9] as early as 1977. At the wavelength 436 nm it has a  $0.8 \lambda/\text{NA}$ -value of  $0.8 \mu\text{m}$ . The sum of the refractive powers differs only slightly from that of the previous example; this is also true of all further lenses. The average refractive indices are still quite high and amount to  $n_+ = 1.65$  and  $n_- = 1.73$ . The number of lens elements of the convergent groups has been increased in order to arrive at moderate deflections to new constrictions at the sites of strong bulges. The aperture rays can be well corrected by these moderate deflections without causing excessive strain in the lens. Low-power lens elements are favorable for production and assembly. The difficulties in the manufacture of such lenses are described in papers by Janusz Wilczynski [10], Anthony Phillips and John Buzawa [11]. I shall not discuss the problems here because it is well known that such lenses are difficult to manufacture. Relaxed optical systems are therefore of paramount importance in this field.

A lens designer must choose which of the two ways he wants to follow to solve a specific problem:

1. Are higher-order aberrations to be compensated by suitable means of correction?
- or,
2. Are higher-order aberrations to be prevented from occurring?

The compensation of a higher-order aberration means additional strain which in turn produces aberrations of still higher order, although it permits the production of short lenses. The lenses will be longer when the second way is followed, because every Seidel coefficient must be kept small to prevent higher-order aberrations from occurring. That means that all surfaces must be relaxed, which calls for a great number of low-power lens elements or components effective over long distances.

The design of the convergent front part with the strongest bulge in Fig. 5 is similar to that I showed in 1975 [6,7] of long, high-aperture retrofocus lenses for 16 mm and 35 mm film. These lenses are characterized by a great physical length in relation to the focal length. The second bulge of the rear ray bundle did, however, not exist at the time or was only indicated.

#### Double-bulge lenses

Fig. 6 (Zeiss S-Planar  $f/1.3\text{-}65 \text{ mm}$ ) shows an advanced model of this lens, again for a large image field. In this lens and all following items a divergent lens in front of the image is effectively utilized for further field flattening. A distinct working distance is still left. This and all following lenses are new with overall lengths around  $8f$ . In practice this overall length covers almost half the object-to-image distance at an image scale of 1:10.

The great physical length increases the distances between the lenses' principal planes and reduces the focal length at the same object-to-image distance. Compared with the lens S-Planar  $f/1.6\text{-}50 \text{ mm}$  (Fig. 4) the focal length is reduced by about 25%. Because of the telecentric ray path at the image side, the result of identical image height will always be larger angular fields in front, which is of disadvantage, though, for the permissible tolerances of the mask position. The tolerances which apply there to the tilt angle (the result is asymmetric distortion) and defocusing (the result is a change in the image scale) must thus be tightened by 25%. It is possible, though, to keep within these tolerances.

When we designed lenses for microlithography we wanted to keep the distortion below  $\pm 0.1 \mu\text{m}$ . Short lenses did not present any problem in this respect, whereas the performance of long lenses was limited by fifth-order distortion as the overall length increased. For large fields the overall length of such lenses and thus the double bulge of the ray bundle cannot be further increased. This is true of the lens discussed here and all following ones. Distortion is negative in the image zone and positive at

the edge of the image.

Fig. 6 shows the Zeiss S-Planar  $f/1.3\text{-}65 \text{ mm}$  for a wafer stepper made by Censor for an object-to-image distance of 1004 mm. The wavelength is 436 nm, the aperture 0.35, and the effective field size  $10 \times 10 \text{ mm}^2$ . The value of  $0.8 \lambda/\text{NA}$  is  $1 \mu\text{m}$ . An analysis of the contribution of the lens' four parts to the total refractive power (weighted power) and to the total sum of all refractive powers reveals that both convergent parts contribute.

This applies even more to the lens shown in Fig. 7, although the effect of the divergent front part will always be greater. These two items are the first examples of lenses with two-times considerably increased  $\omega$ -values. You will see how this enables us to maintain the  $\lambda/\text{NA}$ -value with low-index glasses of satisfactory transmission. The average refractive indices of these two examples are virtually as high as before, i.e.  $n_+ = 1.64$  and  $n_- = 1.73$ .

However, the shorter object-to-image distance of 602 mm of the Zeiss S-Planar  $f/1.3\text{-}36.5 \text{ mm}$  (Fig. 7) allows already the use of the working wavelength 405 nm. According to the value of  $0.8 \lambda/\text{NA}$  ( $\text{NA} = 0.35$ ) features of  $0.9 \mu\text{m}$  should be realizable in practice.

Despite long paths in glass the net transmittance is still above 80%. The net transmittances Schott glass works, Mainz give in their catalog were used for the calculations. I should like to emphasize in this connection the great importance of glass types with better transmission characteristics for the design of optical systems for microlithography. This applies to high-index lanthanum and dense flint glasses used so far, as well as to the classical glass types which were employed for the lenses described below down to the working wavelength 365 nm. These lenses could only be realized thanks to the excellent transmittance of Schott glasses such as BaK 5, UBK 7, FK 5 of which the convergent lenses are made, and some flints of the divergent lenses which are kept as thin as possible.

The next example is the Zeiss S-Planar  $f/1.38\text{-}64 \text{ mm}$  (Fig. 8). It has been extended by one lens element, because the high-index glasses had to be abandoned in order to arrive at high transmittance at the same wavelength of 405 nm but at the long object-to-image distance of 1004 nm. The lens features an additional convergent lens in the convergent rear group. This guarantees the same moderate second constriction with low refractive indices than with the previous high ones. The convergent front part has been maintained. An aperture reduced to 0.33 compensates the lower refractive



indices and stronger curvatures of the surfaces. With these wavelength and aperture values it should be possible in practice to obtain 1  $\mu\text{m}$  features in a 10x10 mm<sup>2</sup> field. The average refractive index of the convergent lenses is only 1.55, that of the divergent ones 1.64. We thus reached our goal of using classical glass types.

The above also applies to the last example, the Zeiss S-Planar f/1.44-37 mm (Fig. 9) for the shorter object-to-image distance of 602 mm and corrected for the wavelength 365 nm. The aperture is 0.315 and the value of 0.8  $\lambda/\text{NA}$  again 0.9  $\mu\text{m}$ .

Compared with the lens shown in Fig. 7 for the wavelength 405 nm, the depth of focus is increased by 11%; it would be 19% higher for a lens for 436 nm with the same value of  $\lambda/\text{NA}$ . These values do not seem to be high. But even minor gains are valuable considering the little depth of focus of these lenses – according to the Rayleigh criterion it is  $\pm 1.3 \mu\text{m}$  in the last example – the efforts which must be made in production to maintain this depth of focus over the entire field, and how accurately the silicon wafers must be flattened and aligned. The matter is further complicated by features which in microlithography must be produced at a certain depth and even across steps.

The angular field could also be increased as the development advanced. That of the last lens is greater by 33% than in the preceding example (Fig. 8). About half of this increase is due to an additional cemented surface of the front component, which limits the fifth-order distortion. It is a means to correct higher-order aberrations. But as it produces strain I try to avoid its use. I have not yet found relaxing means, though. This cemented surface produces negative distortion by a small jump in the refractive index and a strong curvature. The distortion affects particularly great image heights. However, the fifth-order distortion remains the limiting aberration. According to the Rayleigh criterion the effective band widths around the different working wavelengths of the lenses for microlithography discussed here range from  $\pm 6 \text{ nm}$  to  $\pm 10 \text{ nm}$ . In spite of long paths in glass the net transmittances remain above 80%.

### Conclusion

A first insight is given by the two simple relations  $\sum \varphi$  small and  $\sum F = 1$ . Table 1 gives a survey of the nine lenses discussed above.

You will have noticed that the line of lenses with typical double-Gauss characteristics also includes one item with typical retrofocus properties. In retro-

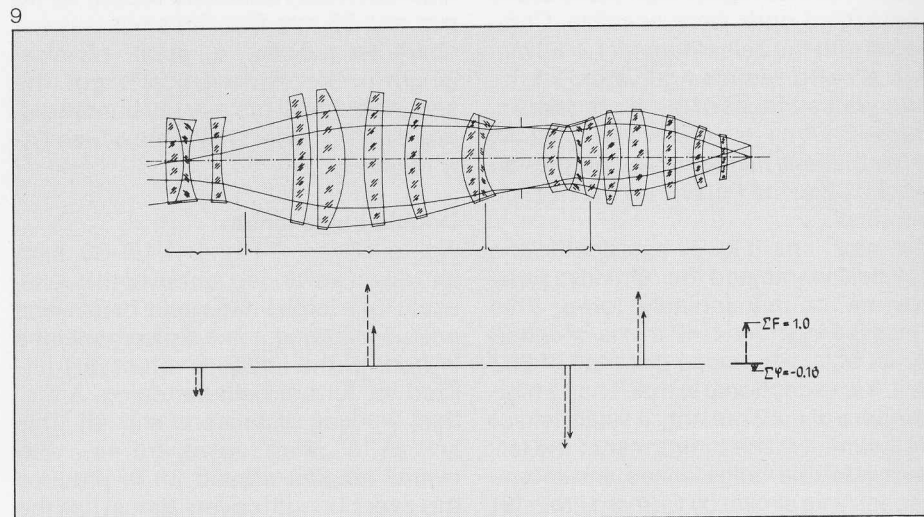
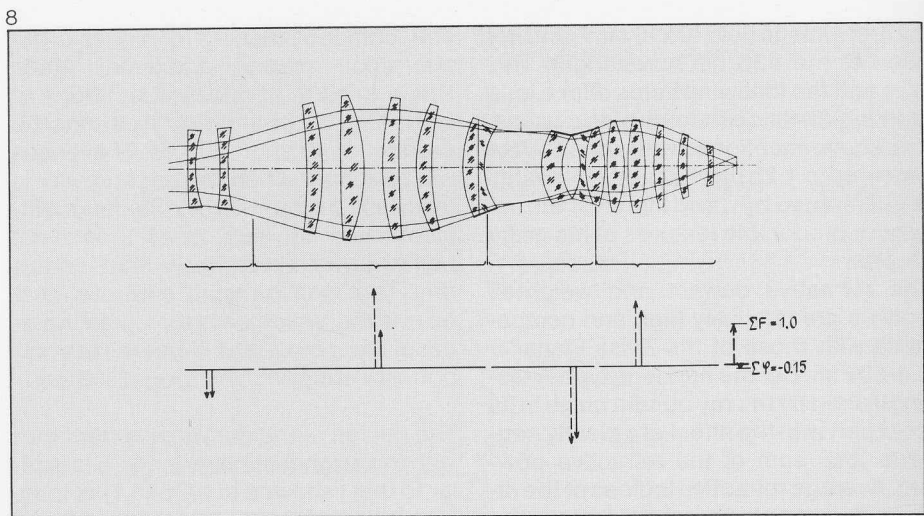


Fig. 8  
Zeiss S-Planar f/1.38-64 nm for  $\lambda = 405 \text{ nm}$ .

Fig. 9  
Zeiss S-Planar f/1.44-37 mm for  $\lambda = 365 \text{ nm}$ .

	$\sum \varphi_i$	$n_+$	$n_-$	Petzval sum
Planar f/1.4-50	0.46	1.78	1.72	0.17
Planar f/0.7-50	0.27	1.70	1.65	0.10
Distagon f/1.2-18	0.07	1.67	1.74	0.10
S-Planar f/1.6-50 $\lambda = 436 \text{ nm}$	-0.17	1.65	1.72	0.03
S-Planar f/1.1-42 $\lambda = 436 \text{ nm}$	-0.14	1.65	1.73	0.02
S-Planar f/1.3-54 $\lambda = 436 \text{ nm}$	-0.14	1.64	1.73	0.02
S-Planar f/1.3-36.5 $\lambda = 405 \text{ nm}$	-0.15	1.64	1.73	0.02
S-Planar f/1.38-64 $\lambda = 405 \text{ nm}$	-0.15	1.55	1.64	0.02
S-Planar f/1.44-37 $\lambda = 365 \text{ nm}$	-0.16	1.55	1.64	0.02

spect this lens can well be compared with the last-mentioned lenses for microlithography. This evidences again how the developments of different lens types mutually stimulate each other.

The constriction of the lenses and its

influence on the Petzval sum decreases in the sequence the lenses are discussed. Generally speaking, Planar characteristics disappear and Distagon characteristics become more pronounced.

A new feature is the strong double bulge of the ray bundle. According to my experience it is impossible with lenses not featuring these bulges to achieve for large fields a satisfactory transmittance at the wavelength 365 nm, because high-index glasses must be used for correction. The relief is insufficient even when the aperture is lower at shorter wavelengths. With these lenses it is impossible to abandon the high-index glasses for those with better transmission. The reduced aperture of our new lens designs eases correction more than the limited choice of glass types complicates it. This is more pronounced for the wavelength 365 nm vs. 405 nm than for the wavelength 405 nm vs. 436 nm, although only very few glasses can be used for correction at 365 nm. We have reached a limit. In terms of illumination only the three mercury lines (436, 405, 365 nm) can be used as working wavelengths. The shorter wavelengths have the advantage of higher energy. If this limit is to be exceeded in the future, new glass types must be developed by the glass manufacturers or new systems invented by the lens designers, which combine quartz glass and fluorite. Yet, the *Abbe* numbers and refractive indices of these two materials differ only slightly, so that more, new difficulties will arise than experienced when these materials were used separately [12, 13]. The use of still shorter wavelengths will perhaps enable the light-optical techniques in microlithography to keep or even increase the span they are ahead of electron-optical and X-ray procedures.

#### Acknowledgement

Part of the work reported above was supported by the German Bundesminister für Forschungs und Technologie as part of the technology program of his ministry, namely the *Distagon* f/1.2-18mm (NT 1017), *S-Planar* f/1.1-42 mm; f/1.3-65 mm; f/1.3-36.5 mm; f/1.38-64 mm, and f/1.44-37 mm (NT 1071).

#### Summary

Diffraction-limited, high-aperture lenses for large image fields are preferably made of high-index glasses. However, the transmission of high-index glasses is poor. To achieve for such lenses high transmission in the violet (405 nm) or ultraviolet (365 nm) region (to increase the depth of focus, for example) classical low-index glasses must be used. That means, however, that a most valuable means to correct the curvature of field cannot be applied. A new way must be found. According to a classical theorem, "the curvature of field can be reduced by combining positive and negative lenses". (The bundle diameter must be larger at the site of the convergent than of the divergent lenses. See e.g. *Slevogt*, *Technische*

*Optik*, Berlin 1974, p. 233). This measure can be repeatedly employed. The effect will be the more pronounced the greater the ratio of the bundle diameters. A new lens type is presented characterized by two strong bulges of the ray bundle. With this lens aberrations were corrected at the same or even improved value of  $\lambda/NA$  at working wavelengths down to 365 nm for hitherto unattained field sizes at comparable values of aperture, object-to-image distance, telecentric ray path in the image space, etc. In spite of long paths in glass the net transmittance remains above 80%. The lenses must be of long design.

A great number of lenses permits moderate bulges and constrictions of the ray bundle, and results in low-index, relaxed lens components. For still larger fields means must be found to correct the fifth-order distortion of such long lenses.

Underlined words such as *S-Planar* are trade-marks.

#### References

- [1] *Hoogland, J.*, Systematics of Photographic Lens Types, International Lens Design Conference, Oakland 1980.
- [2] *Slevogt, H.*, *Technische Optik*, Walter de Gruyter & Co., Berlin 1974, p. 233.
- [3] *Čanžek, L.*, Anspannung und Zentrierempfindlichkeit im paraxialen Bereich, *Optik* 53, 105-113 (1979).
- [4] *Wöltche, W.*, Optical Systems Design with Reference to the Evolution of the Double-Gauss Lens, International Lens Design Conference, Oakland, 1980.
- [5] *Glatzel, E.*, New Developments in Photographic Objectives, Optical Instruments and Techniques 1969, Oriel Press, Newcastle-upon-Tyne, 407-428 (1970).
- [6] *Fischer, H., E. Glatzel, W. Jahn and H. Zajadatz*, US Patent 4,025,169. German Patent Application 25 14 081, 1975.
- [7] *Glatzel, E.*, Neue Objektivkonstruktionen - neue Korrektionsmittel, *Zeiss-Information* 22, 45-50 (1976) No. 85 and *Zeiss-Information* 23, 24-26 (1977), No. 86. and Novel Lens Design for Motion-Picture Cameras, *SMPTE Journal* 87, 1-5 (1978), No. 1.
- [8] *Rimmer, M.P. and B.R. Irving*, Calculation of Partially Coherent Imagery, International Lens Design Conference, Oakland, 1980.
- [9] *Ittner, G.*, Future Possibilities of Dioptric Lenses in Microelectronics, *SPIE* 100, Semiconductor Microlithography II, 115-119 (1977).
- [10] *Wilczynski, J.S.*, Lenses for Microelectronic Applications, International Lens Design Conference, Oakland, 1980.
- [11] *Phillips, A.R. Jr. and M.J. Buzawa*, High Resolution Lens System for Sub-Micron Photolithography, International Lens Design Conference, Oakland, 1980.
- [12] *Glatzel, E.*, UV-Objektiv 2/50, Bildwinkel = 30°, aus Quarzglas und Flußspat, Korrektionsgang und Korrektionszustand, *Optik* 26, 411-421 (1967).
- [13] *Glatzel, E.*, UV-Objektiv 4/100, Bildwinkel = 41°, aus Quarzglas und Flußspat, Korrektionsgang und Korrektionszustand, *Optik* 30, 354-358 (1970).